# Influences of subway tunneling on disaster of overlying rainwater and sewage pipelines



## Efectos de la construcción de túneles subterráneos como causa de desastre en redes de desagües pluviales y alcantarillados

Yu Hu<sup>1,2</sup>, Aijun Yao<sup>1</sup>, Jiantao Zhang<sup>1</sup> and Haifeng Guo<sup>1</sup>

- <sup>1</sup> Key Laboratory of Urban Security and Disaster Engineering, Ministry of Education, Beijing University of Technology, Pingleyuan 100#, Beijing, 100124, Beijing, China. Email: huyuqcxy@126.com
- <sup>2</sup> College of Civil Engineering, Henan University of Engineering, Zhengzhou, 451191, Henan, China

**DOI:** http://dx.doi.org/10.6036/8661 | Recibido: 23/11/2017 • Evaluado: 23/11/2017 • Aceptado: 16/01/2018

#### **RESUMEN**

- La construcción de túneles puede causar el desastre de los gasoductos circundantes e inducir graves consecuencias, como el colapso de las carreteras. Los estudios pertinentes existentes se centran principalmente en los conductos de presión de pequeño diámetro, mientras que las exploraciones sobre las características de desastre de los conductos de agua de lluvia y de aguas residuales (ORSP: overlying rainwater and sewage pipelines) con gran rigidez y resistencia. Además de los métodos de investigación de las características de desastre de las tuberías de presión de pequeño diámetro, los métodos de investigación son principalmente una combinación de análisis teóricos y experimentales, o una combinación de análisis teóricos y de elementos finitos. Con el fin de estudiar las características de desastre del ORSP de gran diámetro durante la construcción de túneles, se evaluaron las características de asentamiento y tensión de los gasoductos a través de un modelo experimental del programa ortogonal túnel-tubería, y se discutieron las influencias de la construcción de túneles sobre el desastre del ORSP. Luego, la simulación no lineal del modelo se realizó mediante el análisis de elementos finitos. Los resultados numéricos se comparan con los resultados de experimentos de modelos y cálculos teóricos, y se examinaron los principales índices que influyen en las características de desastre de la ORSP. Los resultados demuestran que la curva de asentamiento del ORSP se ajusta a la distribución gaussiana, y la altura del subsidio aumenta con el aumento de los procedimientos de excavación y el tiempo de estabilización, alcanzando los 19,5 mm. La tensión en ORSP es simétrica alrededor de la línea central del túnel. La parte inferior se presiona ligeramente, mientras que la superior se estira localmente. La fiabilidad del modelo numérico y el cálculo teórico es validada por el análisis de elementos finitos. La tensión oscila entre -545-59kPa, indicando que la mayoría de las posiciones de la parte superior e inferior del ORSP soportan bajas presiones. El asentamiento del ORSP según el análisis de parámetros disminuye con el aumento de la distancia entre la red del túnel y la tubería (I) y el diámetro interior de la tubería (d). El asentamiento de ORSP se vuelve estable cuando I/D>3 (D es el diámetro del túnel) y d/I>0,24. El estrés de ORSP disminuye gradualmente con el crecimiento de I y d. Las conclusiones de este estudio pueden proporcionar referencias teóricas para las medidas de protección de ORSP en la construcción de túneles subterráneos.
- Palabras clave: tuberías, experimento modelo, elemento finito, características de desastre, validar.

#### **ABSTRACT**

Tunneling can cause the disaster of surrounding pipelines, thereby inducing serious consequences, such as road collapse. Existing relevant studies mainly focus on small-diameter pressure pipelines, while explorations on disaster characteristics of largediameter overlying rainwater and sewage pipelines (ORSP) with high rigidity and strength as well as socket are rare, and the research methods of disaster characteristics of small-diameter pressure pipelines are mostly a combination of theoretical and experimental analyses, or a combination of theoretical and finite element analyses. In order to study the disaster characteristics of large-diameter ORSP during tunneling, the settlement and stress features of pipelines were evaluated through a model experiment of the pipe-tunnel orthogonal program, and influences of tunneling on the disaster of ORSP were discussed. Then, nonlinear simulation of the model was performed by finite element analysis. Numerical results are compared with model experiment and theoretical calculation results, and main indexes that influence the disaster characteristics of ORSP were examined. The results demonstrate that the settlement curve of ORSP conforms to Gaussian distribution, and the height of subsider increases with the increase in excavation procedures and stabilization time, thereby reaching 19.5 mm. Stress on ORSP is symmetric around tunnel centerline. The bottom is pressed slightly, while the top is stretched locally. Reliability of numerical model and theoretical calculation is validated by the finite element analysis. Stress ranges between -545-59kPa, indicating that most positions of top and bottom of ORSP bear low pressures. The settlement of ORSP according to parameter analysis decreases with the increase in pipe-tunnel net distance (I) and inner diameter of pipeline (d). The settlement of ORSP becomes stable When I/D>3 (D is tunnel diameter) and d/l>0.24. The stress of ORSP gradually decreases with the growth of I and d. Conclusions in this study can provide theoretical references for ORSP protection measures in subway tunnel constructions.

**Keywords:** pipelines, model experiment, finite element, disaster characteristics, validate.

#### 1. INTRODUCTION

Urban mass transit has reached the large-scale construction stage with the rapid economic development in China. Subway construction distributes along urban main roads and thus inevitably runs through urban center regions. Therefore, running

through existing municipal pipelines is necessary. Excavation of subway tunnel can cause deformations of surrounding strata and surface. Excavating influences on rainfall and sewage pipelines beneath the road cannot be neglected and may affect normal use of overlying rainwater and sewage pipelines (ORSP) and cause disaster consequences. Abundant tap water and sewage flow in soil mass may occur, thereby changing structural properties of soil mass and resulting in surface collapse. These consequences can influence normal operation of ground transportation and stability of surrounding rock and earth mass.

In terms of the influences of tunneling on the ORSP in soil mass, Chinese and foreign scholars mainly concentrate in pipeline model, pipe-soil interaction, and pipe displacement and internal forces. Winkler elastic foundation beam model [1-5] views pipelines as the foundation beam and soil mass as a series of independent springs, and studies these problems by determining the coefficient of springs. Bending moment and load of pipelines due to tunneling construction are predicted by appropriate foundation modulus. However, this model is inapplicable to tunnel-pipe-soil interaction. Elastic continuum solution [5-6] is applied to nodal pipelines caused by tunnels and concludes that surface displacement caused by ground loss is consistent with pipeline deformation. Therefore, pipeline deformation can be expressed by Gaussian distribution. The combination of nonlinear soil mass in pipe-soil interaction is crucial when describing ground surface settlement profile [7]. The abovementioned studies mainly focus on small-diameter pressure pipelines. The ORSP in the municipal administration is characterized by high rigidity, highbearing strength and socket at pipe joint. Therefore, no mature studies on disaster mechanism of ORSP caused by tunneling have been reported, thereby causing potential risks for subway tunnels running through large-diameter ORSP.

Influences of subway tunneling on deformation and stress of large-diameter ORSP have to be studied to offset shortages of abovementioned studies. In this study, the disaster mechanism of ORSP during tunneling is discussed by combining theoretical analysis, model experiment, and finite element analysis. Research results establish the analysis of influences of pipe-tunnel distance and inner diameter on pipelines.

#### 2. STATE-OF-THE-ART

Common pipelines, except ORSP, can show different characteristics because of various interfaces and materials. Pipelines suffer complicated stress and unique deformation when traversing tunnels. Currently, scholars achieved abundant studies on factors influencing deformation and stress of pipelines during tunneling construction through simplified theoretical analysis, experiment, and finite element method. These scholars have proposed several prediction formulas. However, they attached considerable attention to pipe deformation, relative rigidity, and stress state. Several models must be constructed to discuss prediction formula by theoretical method, and preset hypotheses cannot be ignored. First, the hypothesis of pipe absence is proposed to estimate ground surface settlement caused by tunneling and then calculate responses of pipelines to settlement stratum. Thus, the disaster of pipelines is studied. For example, Atterwell [1] discussed soil-tunnel interaction through single degree-offreedom load-displacement relation by using the Winkler ground model. However, Klar [8] and Voster [9] believed that this model demonstrates several limitations because this model disregarded the continuous quality of basic deformation. A strict continuum

solution was proposed according to half-space homogeneous model. Klar [10] extended elastic continuum solutions to local yield along pipelines. Moreover, the prediction formula of continuum elastic solution of small-diameter pipe with nodes is proposed [5]. These studies use Winkler elastic foundation beam as the basic model and follow preset hypotheses to discuss stress performance and deformation mechanism of small-diameter pipelines according to half-space characteristics.

Tunnel excavation and pipe-soil interaction cannot be iqnored during an experimental study on pipe deformation and stress. Most studies apply theoretical and finite element analyses, but only a few studies used model experiment [11-13]. Several scholars adopted site monitoring method. However, monitored data exhibit poor universality and are difficult to be verified due to complicated site conditions. Consequently, a model experiment is crucial. Zhu [14] conducted a similarity model experiment by using a model box to simulate semi-automatic device of shield excavation. This experiment could simulate shield excavation well and demonstrate smaller disturbances to experiment results than artificial excavation. Wang [13] established an analysis model for pipeline particle flow based on laboratory experiment and verified experimental phenomenon, thereby concluding that volume lossinfluences pipe-soil relative displacement. Marshal [12] and Voster [11] verified the influences of stratum losses on adjacent pipelines during tunneling by a series of centrifuge experiments. These authors discussed ground surface settlement, pipeline settlement, pipeline bending moment, and shearing strain of soils around the pipeline. These studies also focused on small-diameter pressure pipelines, but few studies discussed ORSP.

Moreover, finite element analysis has become one of the important means and analysis results have been accepted by engineering and academic circles. Marshal [12], Klar [10] and Wang [15] discussed pipeline responses to tunnel excavation by using a series of numerical parameter analysis. The bending moment strain of pipelines was evaluated by dimensionless images. Most finite element simulation analysis and the proposed theoretical analysis or experimental results are verified mutually [16-19]. However, finite element analysis lacks mutual verification by combining theoretical deduction and experiment.

The present study combined theoretical analysis, model experiment, and finite element analysis for verification given the scarcity of existing studies. First, a model computing program was designed. The responses of ORSP to shield the excavation of tunnel construction were studied by the similarity model experiment. Thus, boundary conditions of the model experiment were applied to existing theoretical expression, and the corresponding results were calculated. Finally, the prototype model was established and calculated by Midas GTS-NX finite element software. Positions with large deformation and stress on ORSP were analyzed. The analysis results were compared with model experiment and theoretical analysis results, thus obtaining outcomes in favor of engineering construction.

The rest of this study is organized as follows. Section 3 describes the theoretical prediction, experimental condition, and finite element modeling methods for pipeline deformation and stress. Section 4 analyzes the experimental results concerning deformation characteristics and deformation laws of ORSP, and verifies the validity of the finite element model. The influences of ORSP-tunnel distance and inner diameter of pipelines on the disaster of pipelines are described. Section 5 draws the conclusions.

#### 3. METHODOLOGY

#### 3.1. PREDICTION FORMULA

Subsider can be developed on the ground after tunnel excavation. The influencing factors of tunneling-induced surface deformation can be identified by studying the subsider. Peck[20] proposed the calculation formula of transverse surface settlement on the basis of statistical analysis of measured data of surface settlement surrounding the tunnel. The formula can be expressed as:

$$w(x) = w_{\text{max}} \exp(-\frac{x^2}{2i^2})$$
 (1)

According to the relationship between maximum displacement  $(W_{\max})$  and volume loss  $(V_j)$ , the surface settlement can be expressed as:

$$w(x) = \frac{0.313V_l D^2}{i} \exp(-\frac{x^2}{2i^2})$$
 (2)

where W(x) is a transverse surface settlement on two tunnel sides (where x is distant from the tunnel center),  $W_{\max}$  is the maximum settlement at the tunnel center, x is the transverse distance between the two tunnel sides and the tunnel center, i is the subsider width,  $V_i$  is the volume loss rate, and D is the tunnel diameter. The relationship between pipeline deformation and surface subsider is generally hypothesized when discussing deformation of pipes, which are buried at a certain depth. Han et al [21] reported that subsider width in tunneling engineering is only related to the buried depth of central axis. These researchers proposed a prediction formula of pipeline deformation, which is expressed as:

$$w = \left(\frac{0.313 V_{i}^{p} D^{2}}{K_{p} z_{p}}\right) \exp\left(\frac{-x^{2}}{2K_{p}^{2} z_{p}^{2}}\right)$$
(3)

When the tunnel traverses pipelines vertically, the maximum settlement of underground pipelines is as follows:

$$w_{\text{max}} = \frac{0.313 V_{i}^{p} D^{2}}{i_{p}} = \frac{0.313 V_{i}^{p} D^{2}}{K_{p} z_{p}}$$
(4)

where  $V_l^P$  is the volume loss coefficient of the underground pipeline settlement curve. If the tunnel and underground pipeline have a certain included angle, then  $V_l^P \approx V_l$  when the tunnel traverses the underground pipeline vertically.  $i_P$  is the subsider width and  $z_P$  is the vertical distance between underground pipeline and central axis of the tunnel. The formula for subsider width of the underground pipeline is as follows:

$$K_{p} = \frac{0.313 V_{l}^{p} D^{2}}{w_{\text{max}} z_{p}}$$
 (5)

Attewell et al [22] proposed the cumulative probability curve which describes settlement curve along the tunnel excavation direction. Thus, the formula of deep pipeline displacement is further deduced as follows:

$$w = \left(\frac{0.313V_i^p D^2}{K_p z_p}\right) \exp\left(\frac{-x^2}{2K_p^2 z_p^2}\right) \left[G(\frac{y - y_i}{K_p z_p}) - G(\frac{y - y_f}{K_p z_p})\right]$$
(6)

The stress of pipelines with certain buried depth involves pipe-soil interaction and unloading effect of tunnel excavation. Therefore, Yoo [23] assumed that the total stretching strain of the pipeline buried at the depth of  $z_p$  is composed of buckling and axial strains, which are related to curvature. When the pipeline is perpendicular to the tunnel, the stretching strain of pipelines can be calculated by:

$$\varepsilon_{pwx} = 0.089 \frac{V_p d}{i_n^3} = \frac{0.089 \pi V_l D^2 d}{4i_p^3} = \frac{0.070 V D^2 d}{4K_p^3 z_p^3}$$
(7)

$$\varepsilon_{pux} = \frac{0.036}{z_p} \frac{V_p d}{i_n^2} = \frac{0.036\pi V_l D^2 d}{4z_p i_p^2} = \frac{0.028 V_l D^2 d}{K_p^2 z_p^3}$$
(8)

$$\varepsilon_{pvx} = \frac{0.178RF(\varepsilon_{x})V_{p}}{z_{n}i_{n}} = \frac{0.178\pi RF(\varepsilon_{x})V_{l}D^{2}}{4z_{p}i_{p}} = \frac{0.140RF(\varepsilon_{x})V_{l}D^{2}}{K_{p}z_{p}^{2}}$$
(9)

where  $RF(\varepsilon)$  is the strain reduction factor.

Similarly, Wang [24] expressed the formula of the pipeline angle based on the relation between pipeline deformation and volume loss caused by tunnel excavation when the pipeline and tunnel are perpendicular. The angle is expressed as:

$$\theta_x(p) = 2\arctan\left\{\frac{V_p}{2\pi i(p)^2}\right\}$$
 (10)

According to research results of Jiang [25], the relation can be obtained as:

$$i/i(p) = (1 - \frac{z_p}{z_t})^A \tag{11}$$

where A is generally -0.3, thereby adding equation (11) into equation (10), and then the angle can be expressed as:

$$\theta_{x}(p) = 2 \arctan \left\{ \frac{V_{l} V_{e} (1 - \frac{z_{p}}{z_{t}})^{2A}}{2\pi K_{p}^{2} z_{p}^{2}} \right\}$$
(12)

#### 3.2. EXPERIMENT

## 3.2.1. Determination of similarity factor and manufacturing of model box

to study disaster situations of ORSP during shield excavation of a tunnel under pipe-tunnel orthogonal conditions, a similarity model must be established to simulate pipeline responses. Based on three similarity principles [26–28], the similarity factors of geometric similarity, displacement, stress, elasticity modulus and cohesion are 15:1, and the similarity coefficient between gravity and Poisson's ratio is 1:1.

The model box is composed of tempered glass, polymethyl methacrylate, reference beam and angle iron. Its dimension is  $3 \text{ m} \times 1 \text{ m} \times 2 \text{ m}$  (length×width×height) (Fig. 1 (supplementary material)).

#### 3.2.2. Experiment design

The pipe-tunnel orthogonal experiment program was applied (Fig. 2). Shield tunnel was simulated by the prefabricated stainless steel cylinder tunneling device (Fig. 3 (supplementary material)). The elasticity modulus of stainless steel was 14 GPa. The wall

thickness, diameter, inner diameter, and length of the shield tunnel model were 20, 400, 360, and 1000 mm, respectively. Gypsum pipe material (reinforced) was used as the joint. Diameter, pipe thickness, and buried depth of the pipe top were set 150, 10, and 400 mm, respectively. The four sides and bottom plate of the model box were made of angle iron and fixed by bolts to eliminate influences of boundary effect. Ribs were applied at the joint of the tempered glass to reinforce and confine the lateral deformation of the model box.

#### 3.2.3. Similar experiment materials and measurement device

Experiment strata were made of river sand, iron powder, lime and gypsum. River sand and iron powder were used as aggregates, while lime and gypsum were used as adhesives. The composition of similar materials is summarized in Table I (supplementary material). The parameters of the similar materials are listed in Table II (supplementary material).

Gypsum (reinforcement) was used as the similar material of experimental pipeline model. Compressive strength and elasticity modulus were controlled at 1.34 and 2000 MPa, correspondingly. Vertical pipeline displacement and stresses at pipeline top and bottom were included as experimental measurement items. Pipeline displacement was measured by anchor displacement sensor in the range of 0-100 mm. The measurement accuracy was 0.01 mm. Pipeline stress data were collected by resistance strain gage and DH3816N static strain testing system. Distributions of anchor displacement sensor and resistance strain gages are illustrated in Fig. 4 and Fig. 5 (supplementary material).

#### 3.2.4. Experiment process

(1) The strata were filled to the designed height that was kept static for 24 h to stabilize formation consolidation after pipelines were buried. Then, all of the measurement equipment were de-

Miscellaneous fill
Clayey silt I

Fine sand

Gravel pebbles

Clayey silt II

Gravel

300

(a)

Fig. 2: Pipe-shield tunnel orthogonal program (unit: mm). (a)Section view (b) Aerial view

bugged and initial values were recorded. (2) Shield tunnel was excavated manually by 20 times, at 5 cm for each excavation. A total of 100 cm were excavated. Excavation interval was 10 min and measurement device data were recorded. (3) The model was consolidated for 4, 12, 24, and 48 h under static states after excavating the shield tunnel. Pipeline data at these moments were recorded. Experiment covered 24 steps.

#### 3.3. FINITE ELEMENT ANALYSIS

The finite element analysis software Midas GTS NX was used for modeling analysis. This model selected units, boundary conditions, and gridding method by considering the simulated stratum material and geometric nonlinearity, tunnel shield shell, pipe-concrete contact, concrete-pipe-socket contact, and soil contact. The reliability of the finite element model was verified by comparing experimental and theoretical analysis results.

#### 3.3.1. Material characteristics

Mohr-Coulomb constitutive model was used as the model stratum material. Reinforced concrete pipe section and grouting layer of pipelines and shield tunnel were calculated by using the elastic constitutive model. The parameters are listed in Table III.

#### 3.3.2. Unit size and gridding

Model stratum materials, pipelines, pipe section, and grouting layer were established by entity units. Shield shell was modeled by plate unit. Peripheral soil mass of tunnel was determined more than three times of tunnel diameter length to eliminate boundary effect. Therefore, the model dimension was 60 m×45 m×30 m (length×width×height). The thickness of the pipe section and grouting layer were 150 and 300mm, respectively. The total tunnel length was 45 m.

Joints and other units were gridded through tetrahedral meshing technique because of abundant contact surfaces between adjacent joints. Gridding of pipeline and soil masses in the center and around pipelines by defining linear gradient shall be relatively fine, while the gridding of simulated strata and tunnel distant from pipelines could be relatively sparse.

## 3.3.3. Contact setting and boundary conditions

Adjacent pipeline joints involved many contact surfaces. Contact surfaces were set at pipe joint sockets considering influences of

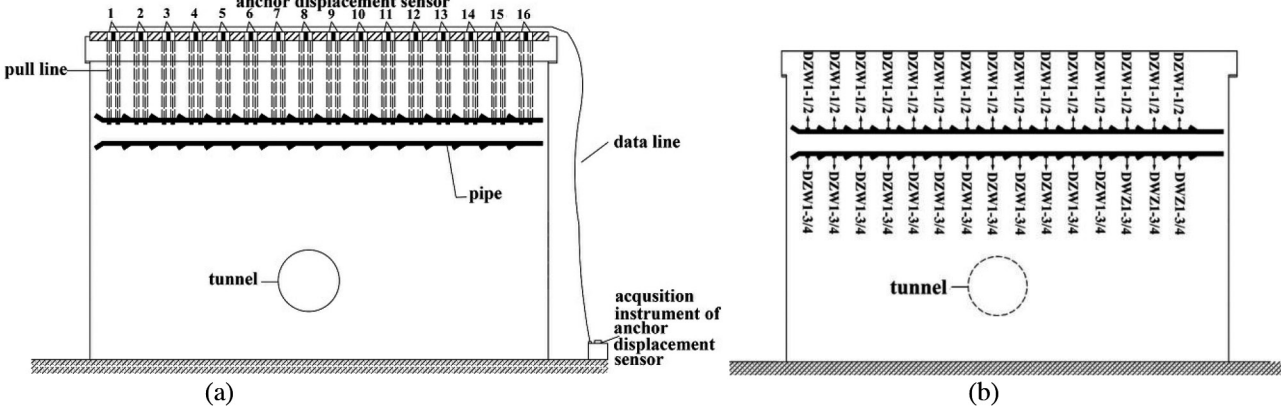


Fig. 4: Displacement monitoring distribution. (a) Profile of resistance strain gage (b) Distribution of strain gage

| Type of rock and soil | Thickness (m) | Elasticity modulus (MPa) | Poisson's ratio | Gravity (kN/m³) | Cohesion/(kN/m <sup>2</sup> ) | Frictional angle (°) |
|-----------------------|---------------|--------------------------|-----------------|-----------------|-------------------------------|----------------------|
| Miscellaneous fill    | 2.55          | 23                       | 0.34            | 16.5            | 0                             | 10                   |
| Clayey silt I         | 5.7           | 18                       | 0.36            | 19.7            | 29                            | 16                   |
| Silty-fine sand       | 4.05          | 26                       | 0.27            | 20.2            | 0                             | 35                   |
| Pebble                | 3.6           | 76                       | 0.26            | 21.5            | 0                             | 40                   |
| Clayey silt II        | 8.1           | 22                       | 0.31            | 19.8            | 30                            | 15                   |
| Pebble                | _             | 74                       | 0.26            | 21.5            | 0                             | 45                   |
| Pipeline              | _             | 30000                    | 0.3             | 25              | _                             | _                    |
| Shield segment        | _             | 34500                    | 0.2             | 25              | _                             | _                    |
| Grouting              | _             | 12000                    | 0.28            | 22              | _                             | _                    |
| Shield shell          | _             | 210000                   | 0.3             | 78              | _                             | _                    |

Table III. Calculated physical and mechanical parameters of the model

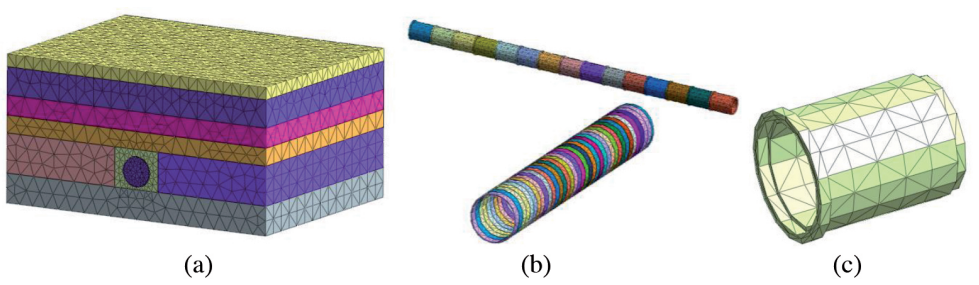


Fig. 6: Components of numerical model gridding. (a) Overall model gridding (b) Relative positions of pipelines and shield tunnel (c) Joint

pipe joint socket. Extrusion and friction effects between adjacent joints were considered. According to Midas GTS help file and related engineering experiences in Beijing, normal and tangential rigidities were 1260 and 900MPa, respectively.

Displacement boundary conditions were set on four sides of the model to confine displacements along the x and y directions. Displacement boundary condition was set at the model bottom to confine movement along the z direction. The upper surface of the model was the earth surface, which was a free boundary. The finite element model is depicted in Fig.6.

#### 3.3.4. Monitoring setting and calculation steps

In this study, two settlement monitoring points were set on each joint to detect front and end displacement of the joint. Four stress monitoring points were set on each joint to study the variations of axial stress at joint interface and middle of joint. The distribution of settlement monitoring points is displayed in Fig. 7, and the distribution of stress monitoring points is presented in Fig. 8. Disaster conditions were evaluated by analyzing the measured data.

#### 3.3.5. Selection of key influencing factors

The effects of net pipe bottom-shield tunnel top distance (J) and inner diameter of the pipeline (d) on vertical settlement and stress of the pipeline were discussed thoroughly. In this experiment, the values of J are 3, 6, 9, 12, 15, 18, 24, and 30 m, and the values of d are 1.2, 1.35, 1.5, 1.65, 1.8, 2.0, 2.2, 2.4, 2.6 and 2.8 m. The distributions of settlement and stress monitoring points are presented in Fig. 7 and 8 (supplementary material).

#### 4. RESULTS ANALYSIS AND DISCUSSION

#### 4.1. MODEL EXPERIMENT RESULT ANALYSIS

#### 4.1.1. Analysis of pipeline displacement

Model experiment results were recovered to engineering prototype. Pipeline displacements at pipe-tunnel intersection

throughout the tunnel excavation and under the stabilization state were recorded (Fig. 9 and 10).

In Fig. 9 (supplementary material), pipeline settlement increases continuously with the growth of shield excavation distance. It reaches the peak (16 mm) at the end of tunnel excavation and can increase to 19.5 mm at 48 h after the stabilization state. In Fig. 10

(supplementary material), pipeline settlement curve displays that the overall pipeline settlement conforms to a Gaussian distribution. The settlements at the two pipe ends are minimal, and the settlements at pipe-tunnel intersection reach the maximum.

#### 4.1.2. Anysis of pipeline stress

model experiment results of pipeline strain were transformed into stress and recovered to the prototype. The mean of top and bottom strains was calculated at the joint above the pipe-tunnel intersection. The stress time-history curve of the joint is illustrated in Fig. 11. Overall stress distributions at pipeline top and bottom are presented in Table IV (supplementary material).

In Fig. 11 (supplementary material), the joint above the pipetunnel intersection is compressed while the shield tunneling continues. The top stress reaches the maximum and then decreases sharply at the 20th excavation procedure (end of excavation). Slight tension occurs at the joint top after stabilization for 48 h. The bottom stress reaches the peak at the 10th procedure (500 mm) and decreases to 0 after stabilization for 48 h. On the basis of data in Table IV, the stress curve is symmetric around the tunnel centerline. Data show slight tension at the joint top above the pipe-tunnel intersection, small compression at pipe top in the range of 1.5 D (D is tunnel diameter), slight tension from 1.5-3 D, and small compression out of 3 D. Significant compression at pipe bottom in the range of 1.5 D (520 kPa up to the most) and small compression in the remaining range are observed. The compression of pipe bottom at the pipe-tunnel intersection is approximately 0, while the remaining sections are compressed to different extents.

### 4.2. VERIFICATION AND ANALYSIS OF FINITE ELEMEMT MODEL

The comparison of pipeline displacement curves from finite element analysis, model experiment and theoretical analysis is depicted in Fig. 12. The comparison of pipeline stress curves from finite element analysis, model experiment, and theoretical analy-

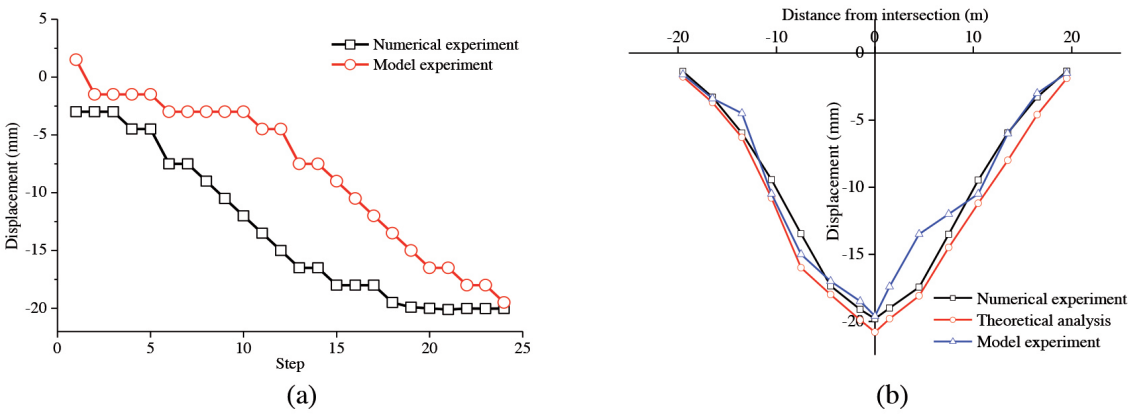


Fig. 12: Comparison of pipeline displacement between model experiment and numerical calculation. (a) Time-history curve of pipeline displacement (b) Vertical displacement of pipeline

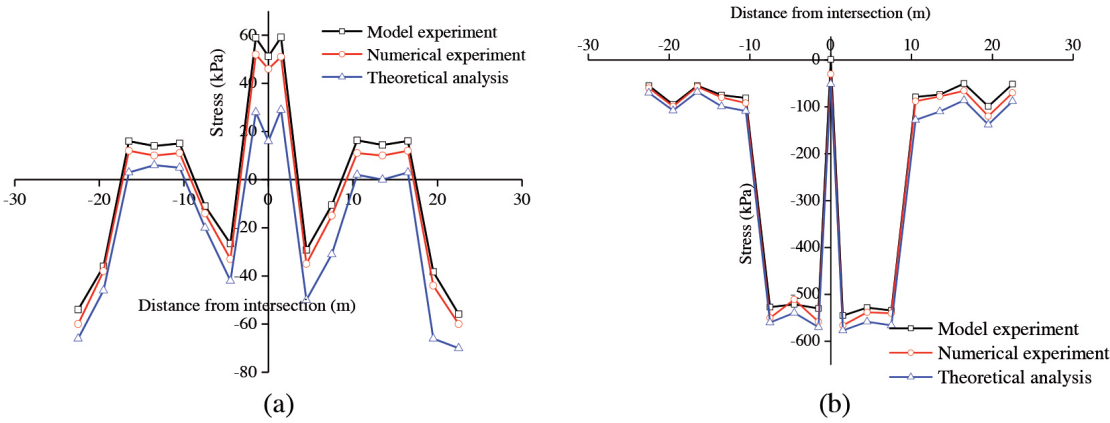


Fig. 13: Comparison of stresses in the pipeline. (a) Comparison of stress on top of the pipeline (b) Comparison of stress at the bottom of pipeline

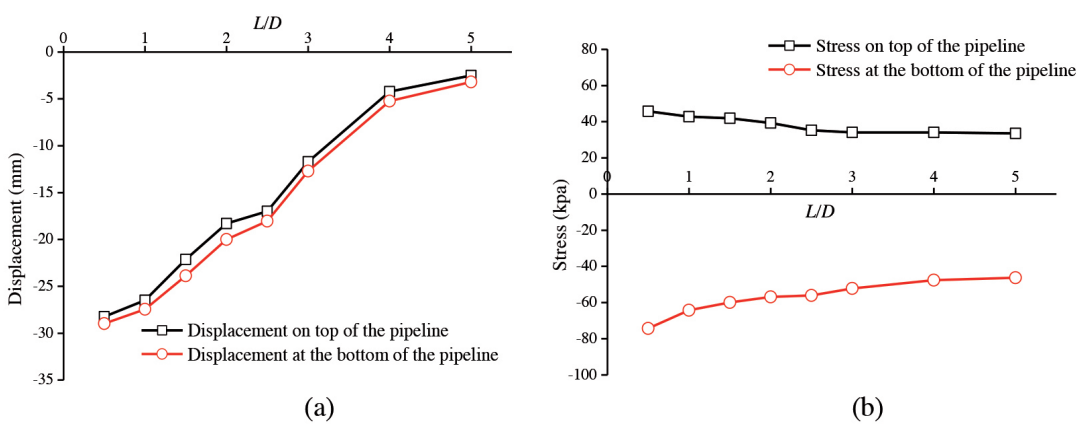


Fig. 14: Effects of pipe-tunnel net distance (I). (a) Vertical displacement of the joint (b) Stress on the joint

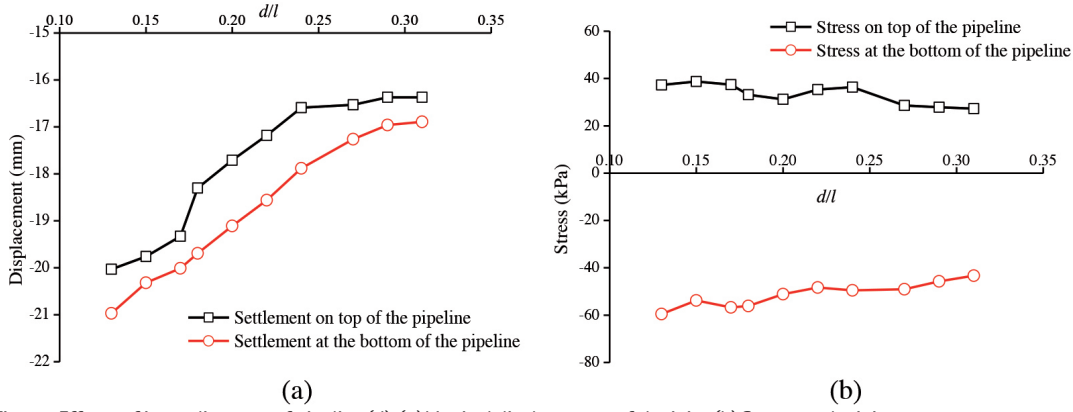


Fig. 15: Effects of inner diameter of pipeline (d). (a) Vertical displacement of the joint (b) Stress on the joint

sis is demonstrated in Fig. 13. The effects of I on vertical displacement and stress of the joint above the pipetunnel intersection are displayed in Fig. 14. The effects of d on vertical displacement and stress of the joint above the pipe-tunnel intersection are shown in Fig. 15.

(1) In the finite element analysis and model experiment, a nonlinear negative relationship between the time-history curve of pipeline settlement and the number of construction procedures was observed, thus indicating the same variation law of pipeline settlement throughout the tunneling process. The final settlement distribution curve agreed well with the theoretical curve during the stabilization process. The pipeline settlement from the finite element analysis deviated for less than 10% with model experiment results and theoretical value, which proved the reasonability of the finite element model.

(2) The pipeline stress curves of the finite element analysis and model experiment conformed to those of empirical theoretical analysis. Minimum pipeline stress was detected near the pipe-tunnel intersection. Results showed minimum compression on top of the pipeline in the range of 1.5 D, slight tension from 1.5-3 D, and minimum compression from 3 D. Significant compression at bottom of the pipe in the range of 1.5

D and minimum compression in the remaining range were observed. The stress curve was symmetric and top stress was smaller than the bottom stress.

- (3) On the basis of calculated results, pipeline settlement decreased continuously with the increase in I/D, and the stress on top and at the bottom of the pipeline decreased slowly.
- (4) The pipeline settlement began to decrease and became stable with the increase in d/l when d/l increased to 0.24. The stress on top and at the bottom gradually changed with the increase in d/l, and a slight reduction in compression.

#### 5. CONCLUSIONS

The settlement and stress distribution curves of ORSP under pipe-tunnel orthogonal conditions are analyzed by combining theoretical analysis, model experiment, and finite element analysis to discuss the disaster characteristics of large-diameter ORSP during tunnel excavation. The influencing laws of pipe-tunnel net distance and inner diameter of the pipeline on the ORSP are summarized. The follows conclusions are drawn:

- (1) The settlement of ORSP conforms to Gaussian distribution throughout the subway tunnel excavation. The subsider height is positively related with excavation progress and stabilization time. Volume loss can influence the pipeline settlement significantly. The settlement of ORSP can be relieved effectively by decreasing volume loss rate by improving shield construction quality.
- (2) The stress concentration on the ORSP throughout the tunnel excavation is observed. The stress on ORSP during the stabilization state is symmetric around the tunnel centerline. The top stress curve is relatively complicated, thereby indicating a slight dislocation between joints. Bottom stress is relatively simple. The bottom stress of ORSP is negatively correlated with pipe-tunnel distance.
- (3) The settlement and stress of ORSP are negatively correlated with *I* and *d*. In particular, the influence on ORSP can be weak when the pipe-tunnel distance and inner diameter (rigidity) are large.

In this study, the settlement and stress curves of ORSP are verified and agree considerably. The influences of pipe-tunnel net distance and inner diameter of pipelines on ORSP are presented. The study results provide a certain technological support to discuss the ORSP damages caused by shield tunnel construction. However, this study only analyzes a single tunnel excavation under pipe-tunnel orthogonal conditions, thus limiting the influencing factors. Further studies involving other influencing factors are still required.

#### **BIBLIOGRAPHY**

- [1] Attewell PB, Yeates J, Selby AR. "Soil Movements Induced by Tunneling and their Effects on Pipelines and Structures". New York: Methuen, Inc., NY. 1986. p. 122–145.
- [2] Vesic AB, 1961. "Bending of beams resting on isotropic elastic solid". Journal of the Engineering Mechanics Division. April 1961. Vol.87-2. p. 35–53.
- [3] Kla A, Vorster TEB, Soga K, Mair RJ. "Soil-pipe interaction due to tunneling: comparison between Winkler and elastic continuum solutions". Journal of Geotechnique, Janurary 2005. Vol. 55-6. p. 461-466. DOI: http://dx.doi.org/10.1680/geot.2005.55.6.461
- [4] Yu J, Zhang C, Huang M. "Soil-pipe interaction due to tunneling: assessment of Winkler modulus for underground pipelines". Journal of Computers and Geotechnics. May 2013. Vol. 50. p. 17–28. DOI: http://dx.doi.org/10.1016/j.compgeo.2012.12.005
- [5] Klar A, Marshall AM. "Shell versus beam representation of pipes in the evaluation of tunneling effects on pipelines". Journal of Tunneling and Underground Space Technology. July 2008. Vol. 23-4. p. 431–437. DOI: http://dx.doi.org/10.1016/j.tust.2007.07.003
- [6] Klar A, Marshall AM. "Linear elastic tunnel pipeline interaction: the existence and consequence of volume loss equality". Journal of Géotechnique. July 2015. Vol. 65–9. p. 788–792. DOI: http://dx.doi.org/10.1680/geot.14.P.173

- [7] Saiyar M, Ni P, Take WA., Moore ID. "Response of pipelines of differing flexural stiffness to normal faulting". Journal of Geotechnique. April 2016. Vol. 66-4. p. 275–286. DOI: http://dx.doi.org/10.1680/jqeot.14.P.175
- [8] Klar A, Vorster TE, Soga K, Mair RJ. "Soil-pipe interaction due to tunneling: comparison between Winkler and elastic continuum solutions". Journal of Geotechnique. January 2005. Vol. 55-6. p. 461–466. DOI: http://dx.doi.org/10.1680/qeot.2005.55.6.461
- [9] Vorster TE, Klar A, Soga K, Mair RJ. "Estimatingtheeffectsof tunneling on existing pipelines". Journal of Geotechnical and Geoenvironmental Engineering. November 2005. Vol. 131-11. p. 1399–1410. DOI: http://dx.doi.org/10.1061/(ASCE)1090-0241(2005)131:11(1399)
- [10] Klar A, Vorster TE, Soga K, Mair RJ. "Elastoplasticsolution for soil-pipe-tunnel interaction". Journal of Geotechnical and Geoenviron-mental Engineering. July 2007. Vol. 133-7. p. 782-792. DOI: http://dx.doi.org/10.1061/(ASCE)1090-0241(2007)133:7(782)
- [11] Vorster TE. "The effects of tunneling on buried pipes". Doctoral dissertation. University of Cambridge, 2006.
- [12] Marshall AM, Klar A, Mair RJ. "Tunneling beneath buried pipes: view of soil strain and its effect on pipeline behavior". Journal of Geotechnical and Geoenvironmental Engineering. December 2010. Vol. 136-12. p. 1664–1672. DOI: http://dx.doi. org/10.1061/(ASCE)GT.1943-5606.0000390
- [13] Wang ZX, Miu LC, Wang RR, et al. "Physical model study on subsurface settlement by tunnelling in sand". China Civil and Engineering Journal. May 2014. Vol. 47–5. p. 133– 139. DOI: http://dx.doi.org/10.15951/j.tmgcxb.2014.05.001
- [14] Zhu YT, Zhang H, Zhang ŽX, et al. "Physical model test study of influence of advance of shield tunnel on adjacent underground pipelines". Journal of Rock and Soil Mechanics. October 2016. Vol. 37-2. p. 151-160. DOI: http://dx.doi.org/10.16285/j.rsm.2016.S2.018
- [15] Wang Y, Shi J, Ng CWW. "Numerical modeling of tunneling effect on buried pipelines". Canadian Geotechnical Journal. July 2011. Vol. 48-7. p. 1125–1137. DOI: http://dx.doi. org/10.1139/t11-024
- [16] Wu FB, Jin H, Shang YJ. "Underground pipeline deformation prediction around urban rail transit tunnel engineering". Chinese Journal of Rock Mechanics and Engineering. July 2013. Vol. 32–S2. p.3592–3601.
- [17] Sun YK, Wu WY, Zhang TQ. "Analysis on the Pipeline Settlement in Soft Ground Induced by Shield Tunneling across Buried Pipeline". China Railway Science. January 2009. Vol. 30-1. p. 80-85. DOI: http://dx.doi.org/10.3321/j.issn:1001-4632.2009.01.014
- [18] Sun HX, Zhao W, Wang ZY. "Monitoring and numerical simulation of underground pipeline settlement during shield tunneling construction". Journal of Shenyang University of Technology. August 2010. Vol. 32-4. p. 454-458.
- [19] Xiao WH. "Research on the Deformation of Soil Induced by Shield Tunnel and Effect on Underground Pipeline". Masteral dissertation. Huazhong University of Science and Technology, 2007.
- [20] Peck RB. "Deep excavations and tunneling in soft ground". Proceedings of 7th International Conference of Soil Mechanics & Foundation Engineering. Mexico: Balkema AA 1969. p. 225-290.
- [21] Han X, Li N, Standing JR. "Study on subsurface ground movement caused by urban tunneling". Journal of Rock and Soil Mechanics. March 2007. Vol. 28–3. p. 23–29. DOI: http://dx.doi.org/10.3969/j.issn.1000-7598.2007.03.033
- [22] Attell PB, Woodman JP. "Predicting the dynamics of ground settlement and its derivatives caused by tunneling in soil". Ground Engineering. November 1982, Vol. 15-8. p. 13-22.
- [23] Yoo C, Kim JH. "A web-based tunneling -induced building/utility damage assessment system TURISK". Tunneling and Space Technology. November 2003. Vol. 18-5. p. 497-511. DOI: http://dx.doi.org/10.1016/S0886-7798(03)00067-1
- [24] Wang T. "Influence and Control of Metro Construction with Mining Method on Adjacent Pipelines". Doctoral dissertation. Beijing JiaoTong University, 2008.
- [25] Jiang XL, Zhao ZM, Li Y. "Analysis and calculation of surface and subsurface settlement trough profiles due to tunneling". Rock and Soil Mechanics. October 2004. Vol. 25–10. p.1542–1544. DOI: http://dx.doi.org/10.16285/j.rsm.2004.10.006
- [26] Lin YM. "Experimental rock mechanics". Beijing: China Coal Industry Publishing House, 1984.
- [27] Prasad SK. Towhata I. "Shaking table tests in earth quake geotechnical engineering". Current Science. November 2004. Vol. 87-10. p.1398-1404.
- [28] Lin G, Zhu T, Lin B. "Similarity technique for dynamic structural model test". Journal of Dalian University of Technology. January 2000. Vol. 40-1. p. 1-8. DOI: http://dx.doi. org/10.3321/j.issn:1000-8608.2000.01.001

#### **APPRECIATION**

This study was supported by the National Natural Science Foundation of China, No. 51578023.

#### SUPPLEMENTARY MATERIAL

https://www.revistadyna.com/documentos/pdfs/\_adic/8661-1.pdf

